

Quantum coherence of Hard-Core-Bosons and Fermions : Extended, Glassy and Mott Phases

Ana Maria Rey^{1,2}, Indubala I. Satija^{2,3} and Charles W. Clark²

¹ *Institute for Theoretical Atomic, Molecular and Optical Physics, Cambridge, MA, 02138, USA*

² *National Institute of Standards and Technology, Gaithersburg MD, 20899, USA and*

³ *Dept. of Phys., George Mason U., Fairfax, VA, 22030, USA*

(Dated: September 16, 2017)

We use Hanbury-Brown-Twiss interferometry (HBTI) to study various quantum phases of hard core bosons (HCBs) and ideal fermions confined in a one-dimensional quasi-periodic (QP) potential. For HCBs, the QP potential induces a cascade of Mott-like band-insulator phases in the extended regime, in addition to the Mott insulator, Bose glass, and superfluid phases. At critical filling factors, the appearance of these insulating phases is heralded by a peak to dip transition in the interferogram, which reflects the fermionic aspect of HCBs. On the other hand, ideal fermions in the extended phase display various complexities of incommensurate structures such as devil's staircases and Arnold tongues. In the localized phase, the HCB and the fermion correlations are identical except for the sign of the peaks. Finally, we demonstrate that HBTI provides an effective method to distinguish Mott and glassy phases.

Recent developments in the manipulations of ultra-cold atoms in optical lattices have opened new possibilities for exploring the richness and complexity of strongly-correlated systems. A particular topic of continuous theoretical interest in condensed matter physics has been the different phases induced by the interplay between disorder and interactions [1, 2]. In cold atomic gases disorder can be introduced in a controlled manner either by placing a speckle pattern on the main lattice or by imposing a quasiperiodic (QP) sinusoidal modulation on the original lattice by using an additional weaker lattice with the desired wavelength ratio [3]. Furthermore, by changing the depth of the optical potential it is experimentally possible to control the effective dimensionality as well as the ratio between atomic kinetic and interaction energy in these systems. All these attributes have made cold atomic systems a unique new laboratory to test many established results, explore new phenomena underlying disordered systems and to confront open questions [4, 5].

In this paper, we use two and four point correlation functions to compare and contrast the different quantum phases in a gas of one dimensional (1D) hard core bosons (HCBs) and fermions subject to a QP potential. In an HCB gas [6], the repulsive interactions between bosons mimic the Pauli exclusion principle, and as a result HCBs resemble in many respects a system of non-interacting fermions. A 1D HCB gas in a periodic optical lattice has just recently been experimentally realized [7]. A system of non-interacting fermions might be realized experimentally by reducing interatomic interactions via Feshbach resonances [8]. Here we treat the case of atoms confined by a periodic lattice, with an additional QP potential introduced to add pseudo-random disorder. A QP system is in between periodic and random systems and is known to exhibit localization transitions at a finite depth of the additional lattice [9]. Here we show that the interplay between the effects of disorder, interactions and quantum statistics leads to new quantum phases, fractal structures such as the devil's staircase, and fragmented Fermi distribution functions. Our studies reveal these effects are manifested in first- and second-order interferometry, which makes them accessible to direct

experimental observation. Furthermore, we find that QP disorder can be exploited to distinguish Mott from glassy phases.

Four-point correlations can be experimentally probed by Hanbury-Brown-Twiss interferometry (HBTI) [10] which measures the intrinsic quantum noise in intensity measurements, commonly referred to as *shot noise* or *noise correlations*. HBTI is emerging as one of the most important tools to provide information beyond that offered by standard momentum-distribution based characterization of phase coherence. The latter is obtained from images of the density distribution of the atomic sample after its release from the confining potential. HBTI is performed by measuring the density-density correlations in such images [11, 12]. Sharp peaks (dips) in these correlations reflect bunching (anti-bunching) of bosons (fermions), characterize the underlying statistics, and reveal information about the spatial order in the lattice [11, 13].

In our study we find that the QP potential induces in the HBTI pattern an hierarchical set of peaks appearing at the reciprocal lattice vectors of both lattices with competing periodicities. We use these peaks together with the first order Bragg peaks in the momentum distribution to provide a detailed characterization of the different many-body phases. Three characteristic phases are known in disordered HCB systems [14]: i) the incompressible Mott Insulator (MI) phase, ii) the superfluid phase, and iii) the insulating but compressible Bose-glass (BG) phase. Here we also find a number of *Mott-like band insulator* phases. These phases correspond to the filling of the sub-bands of a fragmented energy spectrum that emerges from the QP superfluid phase. Transitions to these phases are signaled by a decrease in the intensities of the first and second order coherent peaks. They are found to be followed by a peak to dip transition in the HBTI pattern when an empty band is populated with few atoms.

Ideal fermions in the localized MI and glassy phases exhibit first- and second-order interference patterns similar to the ones of HCBs, except for a different sign of the peaks. However, in the extended phase, fermions and HCBs behave quite differently, with fermion interference patterns displaying vari-

ous complexities of incommensurate structures. When plotted as a function of the filling factor, their quasi-momentum distribution displays an Arnold tongue-like structure; the intensity of HBTI peaks exhibits a step-like pattern which resembles a devil's staircase [15]. Thus, our study points out the potential of ultra-cold gases to provide laboratory demonstrations of non-linear and multi-fractal phenomena.

In a typical experiment, atoms are released by turning off the external potentials. The atomic cloud expands, and is photographed after it enters the ballistic regime. Assuming that the atoms are noninteracting from the time of release, properties of the initial state can be inferred from the spatial images [11, 13, 16]: the column density distribution image reflects the initial quasi-momentum distribution, $n(Q)$, and the density fluctuations, namely the *noise correlations*, reflect the quasi-momentum fluctuations, $\Delta(Q, Q')$,

$$\hat{n}(Q) = \frac{1}{L} \sum_{j,k} e^{iQa(j-k)} \hat{\Psi}_j^\dagger \hat{\Psi}_k, \quad (1)$$

$$\Delta(Q, Q') \equiv \langle \hat{n}(Q) \hat{n}(Q') \rangle - \langle \hat{n}(Q) \rangle \langle \hat{n}(Q') \rangle. \quad (2)$$

In Eq. (2) we have assumed that both, Q, Q' lie inside the first Brillouin zone. In this paper we focus on the quantity $\Delta(Q, 0) \equiv \Delta(Q)$. L is the number of lattice sites and a the lattice constant. $\hat{\Psi}_j$ is a bosonic or fermionic annihilator operator at the site j . The low energy physics of a 1D gas of strongly correlated bosons in an optical lattice modulated by a QP potential is well described by the Hamiltonian:

$$H^{(HCB)} = -J \sum_j (\hat{b}_j^\dagger \hat{b}_{j+1} + \hat{b}_{j+1}^\dagger \hat{b}_j) + \sum_j V_j \hat{n}_j, \quad (3)$$

where \hat{b}_j is the annihilation operator at the lattice site j ; it satisfies bosonic commutation relations, plus the on-site condition $\hat{b}_j^2 = \hat{b}_j^{\dagger 2} = 0$ which suppresses multiple occupancies. Here J is the hopping energy between adjacent sites, and we have introduced $V_j = 2\lambda \cos(2\pi\sigma j)$ to describe the additional QP potential. The parameter λ is proportional to the intensity of the lasers used to create the QP lattice [3]. Note that the primary optical lattice defines the tight-binding condition, and the QP potential is created by a secondary optical lattice. Ideal fermions are described by the same Hamiltonian, in which the HCB operators are replaced by fermion operators.

For a single atom, the eigenfunctions at site j , $\psi_j^{(n)}$ and eigenenergies $E^{(n)}$ of the Hamiltonian in Eq.(3) satisfy:

$$-J(\psi_{j+1}^{(n)} + \psi_{j-1}^{(n)}) + 2\lambda \cos(2\pi\sigma j) \psi_j^{(n)} = E^{(n)} \psi_j^{(n)}. \quad (4)$$

This is the Harper equation, a paradigm in 1D QP systems [9]. For irrational σ , the model exhibits a transition from extended to localized states at $\lambda_c = J$. Below criticality, all states are extended Bloch-like states characteristic of a periodic potential. Above criticality, all states are exponentially localized and the spectrum is point-like. At criticality the spectrum is a Cantor set, and the gaps form a devil's staircase.

In this letter we treat the case of $\sigma = (\sqrt{5}-1)/2$. In numerical studies, σ is approximated by the ratio of two Fibonacci numbers F_{M-1}/F_M , ($F_1 = F_0 = 1, F_{i+1} = F_i + F_{i-1}$), which describe the best rational approximant to σ . For this rational approximation the unit cell has length F_M and the single-particle spectrum consists of F_M bands and $F_M - 1$ gaps. The gaps occur at half-values of reciprocal lattice vectors, which we label by the Bloch index $Q_n = \pm n\sigma \pmod{1} 2\pi/a$, with n an integer and $Q_n a \in (-\pi, \pi)$. The size of the gaps decreases as n increases. In this paper, we present our results for $\sigma = 55/89$.

In general the phase diagram of interacting bosons with disorder is rather complicated. However the analysis simplifies in the HCB limit, because multiple site occupancies are forbidden and the system is thus "fermionized". The ground state energy of an N -particle HCB system is the sum of the first N single-particle eigenstates, as is the case for ideal fermions. This is why the localization transition occurs at $\lambda_c = J$ in HCB systems. Two-point and four-point correlation functions for HCBs can be expressed as a Töplitz-like determinant involving two-point free fermionic propagators: $g_{lm} = \sum_{n=0}^{N-1} \psi_l^{*(n)} \psi_m^{(n)}$. However, in contrast to the ideal fermion case where a direct application of Wick's theorem can be used to express any correlation function in terms of g_{lm} , for HCBs the calculations are more elaborate because they require the evaluation of multiple determinants [13, 17].

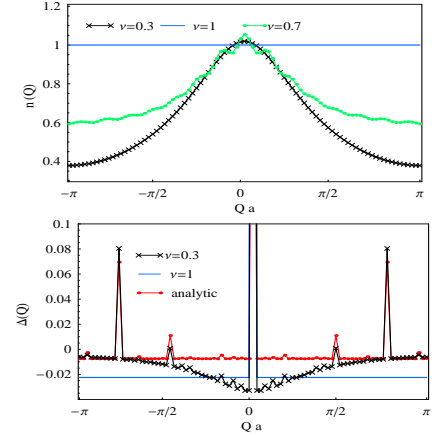


FIG. 1: (color online) Correlations of HCBs in the glassy phase ($\lambda = 2J$) Top: Momentum distribution. Bottom: noise correlations. The central peak at $Q = 0$ is truncated to highlight the QP peaks.

We now discuss the phase diagrams for HCB and fermion systems, starting with the localized phase. In the limit $\lambda \gg \lambda_c$, the single particle wave functions are localized at individual lattice sites, $\psi_j^{(n)} \rightarrow \delta(j-l_n)$ and $E^{(n)} \rightarrow 2\lambda \cos(2\pi\sigma l_n)$, where the localization center l_n is such that $\cos(2\pi\sigma l_{n-1}) < \cos(2\pi\sigma l_n)$. In this limit the determinants involved in the evaluation of HCB correlations become trivial and an analytic description is possible. The momentum distribution interference pattern flattens out for both HCBs and fermions, $\hat{n}(Q) = \nu$ with $\nu = N/L$ the filling factor. The noise correlations

simplify to $\Delta(Q) = \nu\delta_{Q,0} - \frac{2\nu(1-s)}{L} + \frac{(-1)^s}{L^2} \left| \sum_l e^{iaQl} g_{ll} \right|^2$, where $s = 0$ for HCBs and $s = 1$ for fermions. Approximating the sum by an integral, it is possible to show that $\Delta(Q)$ is nonzero only at the reciprocal lattice vectors, Q_n , of the combined superlattice. At these points,

$$\Delta(Q_n) \equiv \Delta_n \approx \nu\delta_{n,0} - \frac{2\nu(1-s)}{L} + \frac{(-1)^s \sin^2[\pi\nu n]}{(\pi n)^2}. \quad (5)$$

Eq. (5) illuminates various important aspects of HBTI in the glassy phase: i) the explicit dependence of noise correlations on quantum statistics, since the boson peaks are positive and the corresponding fermion peaks are negative (except for the autocorrelation peak Δ_0); ii) the potential of HBTI as an experimental spectroscopy tool, since the intensity of the $n = 1$ peak is directly related to the ground state energy of the many-body system, $\Delta_1 = \sum_{k=0}^{N-1} \cos(2\pi n\sigma l_k) = E/(L2\lambda)$; iii) the capability of noise-correlations to clearly distinguish between BG and MI phases, since in the Mott phase, $\nu = 1$, the whole hierarchical set of QP peaks disappears; iv) the universal properties of the peaks whose intensities approach an asymptotic value independently of the underlying commutation relations (except for the Δ_0 peak which is always larger for HCBs). This is a unique feature of the BG phase, as in the extended phase fermionic dips are weaker than the corresponding bosonic peaks (see below).

Fig.1 shows the momentum distribution, $n(Q)$ and noise correlations, $\Delta(Q)$, in the localized phase. Both $n(Q)$ and $\Delta(Q)$ were computed numerically for finite λ using the theoretical framework discussed in Refs. [13, 17]. It should be noted that even though the analytic results were derived for $\lambda \rightarrow \infty$ limit, they provide a fair description of the numerical results for finite λ . The main difference between the $\lambda = 2J$ HBTI pattern and the analytic solution is the negative background which is larger at low quasi-momenta. The background reflects the fact that the single particle localized wave functions have finite localization length $\xi = 1/\log(\lambda)$. This also gives rise to the finite width in the momentum distribution, which is proportional to ξ . As shown in the figure, QP-induced localization may lead to Friedel oscillations [18] in the momentum distribution. These oscillations are due to the two-fold degeneracy of the eigenstates and can be understood in the strongly disordered limit by taking the eigenfunctions to be a superposition of the two degenerate wave functions: one localized at l_k and the other at $L - l_k$. For an odd number of atoms, this leads to $n(Q) = 1 + \frac{1}{L} \cos(2Qa l_{N-1})$.

In the extended phase two-point fermion correlations g_{lm} are long-range, the Töplitz-like determinants are complicated, and we have found an analytical analysis to be difficult. In this phase our numerically obtained results are summarized in Figs. 2 and 3. In contrast to the glassy phase, the momentum distribution exhibits interference peaks which signal the quasi-long-range coherence characteristic of this phase: a large peak at $Q = 0$ and quasiperiodicity induced peaks at reciprocal lattice vectors $\pm\hbar Q_n$ whose intensity depends on the filling factor. These peaks also exist in the noise interference pattern where they are narrower and are accompanied

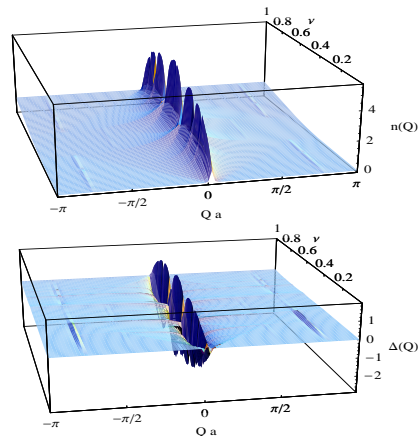


FIG. 2: (color online) HCBs in the superfluid phase, $\lambda = 0.5J$, top: Momentum distribution and bottom: noise correlations where the intensities of the central peaks are scaled by a factor of 1/10 to show the satellite dips.

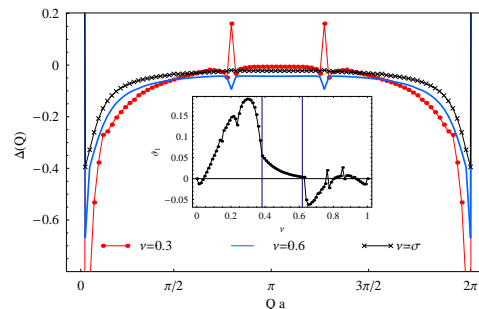


FIG. 3: (color online) HCBs noise correlation for $\lambda = 0.5J$. In the inset we plot the visibility for the dominant peak (see text) as a function of ν .

by satellite dips, immersed in a negative background. The later reflects the long range coherence in the extended phase as discussed in Ref.[13]. It should be noted that, in contrast to glassy phase, few QP related peaks are visible.

A striking aspect of this phase is the cascade of lobes (seen in the Fig. 2) describing a series of transitions to insulating phases. These transitions occur at filling factors $\nu_c^{(n)} = n\sigma(\text{mod } 1)$ and $\bar{\nu}_c^{(n)} = 1 - n\sigma(\text{mod } 1)$, which correspond to the fillings at which the various sub-bands underlying the QP spectrum are completely filled. At these critical fillings, both first and second order correlations depict a reduction in the central peak and dip intensities and also the disappearance of the QP induced peaks as shown in Fig. 2. Explicit computation of the compressibility shows that the system is in fact incompressible at these critical fillings. These features are reminiscent of the Mott insulating phase at $\nu = 1$, so we refer to these phases as *Mott-like band-insulator* phases. However, in contrast to the Mott phase, number fluctuations in these phases do not completely vanish, but are only somewhat reduced.

A rather interesting consequence of the Mott-like band-

insulating transitions is the fact that as ν is increased beyond the critical value, the peaks at the reciprocal lattice vectors associated with the corresponding filled band become dips. This change in the sign of the peaks beyond the critical filling can be seen by plotting the fringe visibility $\vartheta_n = \Delta(Q_n) - [\Delta(Q_n + \delta Q) - \Delta(Q_n - \delta Q)]/2$, with $\delta Q = 4\pi/aL$. Fig. 3 illustrates this for the dominant peaks that occur at $\pm Q_1$. Here the peak to dip transition at $\nu_c^{(1)}$, is signaled by a jump in the visibility from positive to negative. This dip in the second order interference pattern can be interpreted as a manifestation of fermionization. Physical insight into this behavior can be gained by looking at the noise correlation pattern of a single particle which can be shown to exhibit negative fermion-type dips: $\Delta(Q) = |z_0|^2 \delta_{Q0} - |z_Q z_0|^2$ with z_Q is the Fourier-transform of the ground state wave function. For HCBs these negative fringes survive even for two atoms. This implies that the peak to dip transition can be understood as the consequence of an empty band populated with few atoms.

In contrast to the superfluid behavior of HCBs, fermions in the extended phase have metallic properties and different interferometric pattern. For $\lambda = 0$, the sharply peaked HCB momentum distribution is replaced by a step-function profile for fermions: $n(Q) = 1$ for $|Q| \leq Q_F$ and $n(Q) = 0$ for $|Q| > Q_F$, with $Q_F = \pi\nu/a$ being the Fermi momentum. For $0 < \lambda < \lambda_c$ this distribution retains part of the step-like profile of the free fermion gas. However, the Fermi sea gets fragmented and additional step-function structures centered at different reciprocal lattice vectors of the second lattice develop (See Fig.4). We call the filled states centered around $Q = 0$ the main Fermi sea and those around the QP related reciprocal lattice vectors the quasi-Fermi seas.

The quasi-Fermi seas emanating from the QP reciprocal lattice vectors form tongue-like structures which resemble in many respects the Arnold tongues that describe mode-locked periodic windows in the circle map [15]. As the number of atoms increases, the width of the tongues increase. Precisely at the critical fillings $\nu_c^{(n)}$ and $\bar{\nu}_c^{(n)}$, at which a quasi-band is filled up and the system becomes a band-insulator, a quasi-Fermi sea merges with the main Fermi sea. As λ increases, more tongues become visible, and with the increase of ν they overlap in a complex pattern. As seen in Fig.4, we have tongues corresponding to both the particles and holes, which together describe the fragmented Fermi-Dirac distribution when both Q and ν vary.

Noise correlations for fermions (Fig. 4) also bear a striking contrast to those of HCBs (Fig. 2 and 3). One sees a series of plateaus at reciprocal lattice vectors, as ν is varied. The origin of this step-like structure, where jumps occur at the filling factors $\nu_{ju}^{(n)} = |Q_n|a/\pi$, can be understood from a perturbative argument as follows. For non-interacting fermions, for $Q \neq 0$, $\Delta(Q, 0) = -\sum_{k=0}^{N-1} |z_Q^{(k)} z_0^{(k)}|^2$ with $z_Q^{(k)}$ being the Fourier transform of the k^{th} single-particle eigenfunction. For $\lambda = 0$, this overlap between any two different Fourier components is always zero as only the ground ($k = 0$) state has a zero quasi-momentum component, ie, $z_0^{(0)} = 1$. For

small $\lambda \ll J$, first order perturbation theory explains the single step observed at $\nu_{ju}^{(1)} = |Q_1|a/\pi$, as only $z_0^{(k_1)}$ with $k_1 = \nu_{ju}^{(1)}L$ is nonzero. As λ increases further, more steps are observed as other eigenvectors, acquire a nonzero $Q = 0$ component. The steps can also be seen in the $Q = 0$ plane of $n(Q)$. At criticality, the whole hierarchy of steps resembles a devil's staircase, mimicking the multi-fractal structure of the gaps in an energy spectrum that is a Cantor set [9].

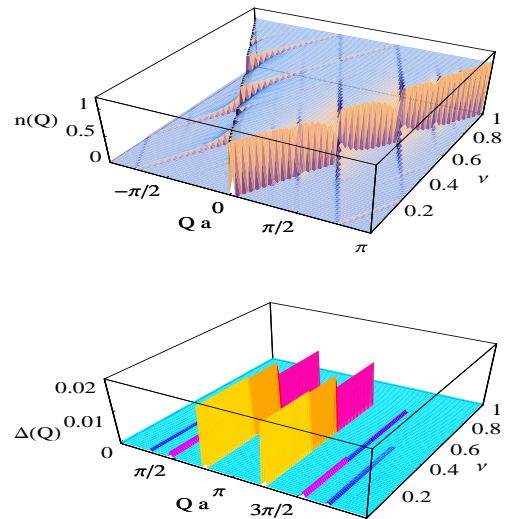


FIG. 4: (color online) Fermions in the metallic phase, $\lambda = 0.5J$. Top: Momentum distribution and Bottom: noise correlations.

In summary, quasiperiodicity can be exploited to distinguish glassy and Mott phases and induce a series of Mott-like band insulating phases. Furthermore, it provides an explicit probe to witness fermionization of bosons, and facilitates the experimental observation of complex fractal structures.

-
- [1] R. Scalettar, G. Batrouni and G. Zimanyi, Phys Rev Letter, **66**, 3144, (1991).
 - [2] J. E. Lye *et al*, Phys. Rev. Lett. **95**, 070401 (2005)
 - [3] K. Drese and M. Holthaus, Phys Rev Letter, **78**, 2932, (1997).
 - [4] D. Jaksch and P. Zoller, New. J. Phys. **5**, 56 (2003);
 - [5] B. Damski *et al*, Phys Rev Letter, **91**, 080403 (2003); K. Osterloh *et al*, Phys Rev Letter, **95**, 010403(2005).
 - [6] M. Girardeau, J. Math. Phys. **1**, 516 (1960).
 - [7] B. Paredes *et al* Nature **429**, 277 (2004).
 - [8] S. L. Cornish *et al*, Phys. Rev. Lett. **85**, 1795 (2000).
 - [9] For a review, see J. B. Sokoloff, Phys. Rep. **126**, 189 (1985).
 - [10] R. Hanbury Brown, R. Q. Twiss, Nature **177**, 27 (1956).
 - [11] E. Altman *et al*, Phys. Rev. A **70**, 013603 (2004).
 - [12] S. Foelling *et al*, Nature **434**, 481 (2005).
 - [13] A. M. Rey, I.I. Satija, and C. W. Clark *cond-mat/0511700* (J. Phys. B in press).
 - [14] M. Fisher *et al*, Phys. Rev. B **40**, 546, (1989).

- [15] E. Ott, *Chaos in Dynamical Systems*, Cambridge University Press, 1993.
- [16] R. Roth and K. Burnett, *Phys Rev A*, **68**, 023604 (2003).
- [17] E. Lieb, T. Schultz and D. Mattis, *Ann. Phys.* **16** (1961) 407.
- [18] J. Friedel, *Nuovo Cimento Suppl.* **7** 287 1958.